Original Articles

Acupuncture and Herbal Medicine

Oridonin mitigates cerebral ischemic–reperfusion injury *via* covalent binding to HMGB1 and inhibiting the HMGB1/TLR4/MyD88/NF-κB signaling pathway

Dandan Liu[1], Shujie Zhang[1], Fei Xia[1], Qiaoli Shi[1], Hui Zhao[2], Yinkwan Wong[3], Yuqing Meng[1], Yanqing Liu[1], Yongping Zhu[1], Xin Chai[1], Jiale Xing[1], Huan Tang[1], Chong Qiu[1], Peili Wang[4,*], Ang Ma[1,*], Jigang Wang[1,*]

[1]State Key Laboratory for Quality Ensurance and Sustainable Use of Dao-di Herbs, Artemisinin Research Center, and Institute of Chinese Materia Medica, China Academy of Chinese Medical Sciences, Beijing, China; [2]School of Traditional Chinese Medicine, Southern Medical University, Guangzhou, China; [3]Department of Physiological Sciences, National University of Singapore, Singapore, Singapore; [4]National Clinical Research Center for Chinese Medicine Cardiology, Xiyuan Hospital, China Academy of Chinese Medical Sciences, Beijing, China

Abstract

Objective: Ischemic stroke (IS) is a leading cause of mortality and disability worldwide, and effective pharmacological treatments are limited. Oridonin (Ori) has demonstrated neuroprotective potential in IS; however, its underlying mechanisms are still poorly understood.

Methods: *In vitro,* oxygen-glucose deprivation/reperfusion (OGD/R) models were established using mouse neuroblastoma Neuro-2a cells and primary cortical neurons. *In vivo,* a transient middle cerebral artery occlusion (tMCAO) model was induced in male C57BL/6J mice to simulate cerebral ischemic–reperfusion (I/R) injury. The key targets of Ori were identified using activity-based protein profiling (ABPP). The binding affinity between Ori and its target protein was validated using multiple approaches, including cellular thermal shift assay (CETSA), molecular docking, and biolayer interferometry (BLI).

Results: Ori significantly suppressed the expression of inflammatory cytokines in tMCAO- and OGD/R-treated neuronal cells. Target identification revealed that high-mobility group box 1 (HMGB1) protein is the key mediator of the protective effects of Ori against cerebral I/R injury. Mechanistically, Ori covalently binds to cysteine (Cys) 106 of HMGB1, reducing its secretion and proinflammatory activity. Additionally, Ori downregulated cytoplasmic HMGB1 levels and the expression of TLR4 and MyD88, as well as the p-p65/p65 ratio in both OGD/R and tMCAO models. Notably, the HMGB1 inhibitor NecroX-7 conferred protection against OGD/R-induced neuronal injury and tMCAO-induced brain damage in mice, which could not be further modulated by Ori treatment.

Conclusions: Our findings demonstrate that Ori confers neuroprotection against brain I/R injury by covalently binding to HMGB1 at Cys106 *via* its reactive carbon–carbon double bonds, thereby eliminating the proinflammatory activity of HMGB1. This molecular interaction reduces HMGB1 secretion and inhibits the downstream HMGB1/TLR4/MyD88/NF-κB signaling pathway, ultimately attenuating neuroinflammation and ischemic damage.

Keywords: Cerebral ischemic–reperfusion injury, Chemical proteomics, HMGB1, Oridonin, Target discovery

Graphical Abstract: https://links.lww.com/AHM/A204

Introduction

Ischemic stroke (IS) results from an abrupt interruption of cerebral blood, leading to acute neurological deficits[1–2]. Current therapeutic strategies, which predominantly involve antithrombotic agents, thrombolytic drugs, and neuroprotective therapies, have substantial limitations with respect to clinical efficacy[3]. Intravenous thrombolysis with tissue plasminogen activator (tPA) remains the gold-standard treatment for acute IS. However, its clinical utility is severely restricted by a narrow therapeutic time window (≤4.5 hours), with fewer than 5% of IS patients benefiting from this therapy[4]. Paradoxically, the restoration of cerebral blood flow following ischemic triggers a cascade of reperfusion injury mechanisms, including hemorrhagic transformation, amplified inflammatory and immune responses, excitotoxic damage, compromised

Dandan Liu, Shujie Zhang, Fei Xia, and Qiaoli Shi contributed equally to this work.

**Corresponding author. Peili Wang, E-mail: wplggyx777@163.com; Ang Ma, E-mail: ama@icmm.ac.cn; Jigang Wang, E-mail: jgwang@icmm.ac.cn.*

How to cite this article: *Liu DD, Zhang SJ, Xia F, Shi QL, Zhao H, Wong Y, Meng YQ, Liu YQ, Zhu YP, Chai X, Xing JL, Tang H, Qiu C, Wang PL, Ma A, Wang JG. Oridonin mitigates cerebral ischemic–reperfusion injury via covalent binding to HMGB1 and inhibiting the HMGB1/TLR4/MyD88/NF-κB signaling pathway. Acupunct Herb Med 2026;6(1):56–72. doi: 10.1097/HM9.0000000000000181*

Received 30 May 2025 / Accepted 22 January 2026

blood–brain barrier integrity, and ultimately, exacerbation of neurological injury[5].

Neuroinflammation is a critical mediator of cerebral ischemic–reperfusion (I/R) injury. Modulating neuroinflammatory responses offers a promising therapeutic strategy for cerebral protection, providing both an extended treatment window and significant therapeutic potential for IS management[6]. During the acute phase of injury, danger-/damage-associated molecular patterns (DAMPs) and proinflammatory cytokines enter systemic circulation, amplifying tissue damage by triggering excessive immune activation. High-mobility group box 1 (HMGB1) is a prototypical DAMP that plays a central role in acute IS pathogenesis[7]. Under physiological conditions, HMGB1 functions as a nuclear protein essential for maintaining genomic homeostasis. However, following cerebral I/R injury, HMGB1 translocates to the extracellular space, where it initiates and amplifies the inflammatory cascade[8]. Given its dual role as both a key mediator of neuroinflammation and a potential biomarker of IS, HMGB1 has emerged as a promising therapeutic target, and HMGB1-targeted strategies may represent a transformative approach to IS therapy[9].

Natural products have demonstrated considerable neuroprotective potential against cerebral I/R injury. However, the precise bioactive constituents, targets, and mechanisms underlying these protective effects remain to be fully elucidated[10]. Donglingcao (*Rabdosia rubescens* [Hemsl.] Hara), also known as poxuedan, is the dried aerial part of this herb used in traditional Chinese medicine[11]. Donglingcao has long been applied to treat various inflammatory conditions, including pharyngitis, laryngalgia, rheumatoid arthritis, and chronic cough[12]. Oridonin (Ori), an ent-kaurene-type tetracyclic diterpenoid isolated from Donglingcao, is the principal bioactive component of this medicinal herb[13]. Extensive pharmacological research has demonstrated that Ori exhibits diverse therapeutic properties, including antitumor, anti-inflammatory, cardioprotective, neuroprotective, and anti-rheumatic effects[14]. Mechanistically, Ori enhances mitochondrial function and antioxidant capacity by activating the Nrf2/HO-1 signaling pathway. It suppresses neuroinflammation by inhibiting activation of the NLRP3 inflammasome and subsequent NLRP3-dependent interleukin-1β (IL-1β) release, thereby ameliorating neural damage in a traumatic brain injury (TBI) model[15]. Furthermore, Ori enhances the phagocytic capacity of BV-2 murine microglial cells while suppressing tumor necrosis factor (TNF)-α and nitric oxide release. Notably, it attenuates BV-2-mediated cytotoxicity in HT-22 murine hippocampal neurons through an NLRP3 inflammasome-independent mechanism[16]. Additional studies have revealed that Ori confers neuroprotection against cerebral I/R injury by specifically inhibiting caspase-9-mediated neuronal apoptosis and excessive mitochondrial autophagy induced by receptor-interacting serine/threonine kinase 3[17]. Nevertheless, the precise molecular targets and mechanisms underlying Ori's neuroprotective effects in cerebral I/R injury require further elucidation.

In this study, we show that Ori confers neuroprotection by significantly downregulating proinflammatory mediators, including IL-1β, IL-6, cyclooxygenase (COX)-2, and inducible nitric oxide synthase (iNOS), in both *in vivo* and *in vitro* models. Using the synthetic derivatives Ori-probe (Ori-p) and hydrogenated Ori (H-Ori), we established that Ori covalently binds to HMGB1 through its reactive carbon–carbon double bonds. Mechanistic studies demonstrate that Ori not only attenuates the proinflammatory activity of HMGB1 but also reduces its secretion, decreases cytoplasmic HMGB1 expression, and suppresses the downstream HMGB1/TLR4/MyD88/NF-κB signaling pathway. These multimodal actions collectively contribute to the robust neuroprotective effects of Ori against oxygen-glucose deprivation/reperfusion (OGD/R)–induced neuronal injury and cerebral I/R damage. Importantly, our findings suggest that the HMGB1-targeting mechanism of Ori represents a promising therapeutic strategy for other HMGB1-driven inflammatory disorders.

Materials and methods

Reagents and kits

The following were used: Ori (HPLC > 98%, Shanghai Yuanye Bio-Technology Co., Ltd., Shanghai, China); Ori-p and H-Ori (synthesized in our laboratory, HPLC > 98%. Their synthetic routes and detailed procedures, as well as characterization data including mass spectrometry results, are available in the Supplemental Digital Content, https://links.lww.com/AHM/A219); DMEM/F12 medium (MeilunBio, PWL005, Dalian, China); Dulbecco's Modified Eagle Medium (DMEM; MeilunBio, MA0212-2); DMEM, No Glucose (MeilunBio, MA0581); Neurobasal-A medium (Gibco, 10888022, Grand Island, NY, USA); poly-L-lysine (PLL; Sigma-Aldrich, P1399, St. Louis, MO, USA); fetal bovine serum (FBS; MeilunBio, PWL217); penicillin-streptomycin (Gibco, 15140122); B27 supplement, serum-free (Gibco, 17504044); cell counting kit-8 (CCK-8; MeilunBio, MA0218); 2% 2,3,5-triphenyltetrazolium chloride solution (TTC; Solarbio, G3005, Beijing, China); 0.25% and 0.05% trypsin digestion solution (Gibco); TMT10plex reagent set (Thermo Fisher Scientific, Waltham, MA, USA); streptavidin beads (Thermo Fisher Scientific); Quantitative Fluorometric Peptide Assay Kit (Thermo Fisher Scientific); sequencing-grade modified trypsin (Promega, Madison, WI, USA); IL-1β (Zen-Bioscience, Chengdu, China), IL-6 (Abclonal, Wuhan, China), COX-2 (Zen-Bioscience), iNOS (Abclonal), HMGB1 (Zen-Bioscience), MyD88 (Proteintech, Wuhan, China), TLR4 (Proteintech), receptor for advanced glycation end products (RAGE; Proteintech), p-p65 (Zen-Bioscience), and p65 (Zen-Bioscience) primary antibodies; mouse TNF-α and HMGB1 enzyme-linked immunosorbent assay (ELISA; Meimian, Shanghai, China) kits; NecroX-7 (MCE, Shanghai, China); recombinant human HMGB1 protein (Abcam, Cambridge, MA, USA); B-box and HMGB1-Cys106 proteins (synthesized in our laboratory).

Instruments

The following instruments were used: Visible fluorescence western blot (WB) imaging system (Azure C400, USA); fluorescence laser scanner (Azure Sapphire RGB

NIR scanner, USA); liquid chromatography-tandem mass spectrometry (LC-MS/MS) (Thermo Fisher Scientific, Orbitrap Fusion Lumis, USA); hypoxic chamber and flow meter (Stemcell Technologies, Vancouver, BC, Canada); enzyme reader (PerkinElmer, Waltham, MA, USA); laser confocal microscope (Leica TCS SP8 SR, Germany); Octet® bios-layer interferometry (BLI) system (Sartorius, Octet-R2, Göttingen, Germany).

Cells

Mouse neuroblastoma Neuro-2a cells and RAW 264.7 macrophages were obtained from Peking Union Medical College and cultured in high-glucose DMEM medium (supplemented with 10% FBS, and 1×10^5 U/L penicillin–streptomycin at 37°C) in a humidified incubator (5% CO_2, 95% air). All experiments were performed using cells between passages 3 and 20 to ensure phenotypic stability.

Primary cortical neuron culture

Primary cortical neurons were isolated from postnatal day 1 (P1) C57BL/6J mice following established protocols[18]. SPF-grade P1 C57BL/6J mice were euthanized by decapitation. The whole brain was rapidly extracted and the cerebral cortex was carefully dissected. The cortical tissue was minced into small pieces and digested in 2 mg/mL papain solution (equal to tissue volume) supplemented with 0.2 mg/mL DNase I for 20 to 30 minutes at 37°C. The enzymatic reaction was stopped by adding 1 mL FBS. The cell suspensions were filtered through 300-mesh sieves and seeded onto PLL-precoated culture dishes in DMEM/F12 (supplemented with 10% FBS). After 4 to 6 hours incubation, the medium was replaced with Neurobasal-A medium (containing B27, GlutaMAX-I additive, and 1×10^5 U/L penicillin–streptomycin). Half of the medium was changed every 2 to 3 days. After 7 days of cultivation, mature neuronal cultures were ready for subsequent experiments.

Animals and transient middle cerebral artery occlusion model

All animal experiments were approved by the Animal Experimental Ethics Review Committee of the Institute of Chinese Materia Medica, China Academy of Chinese Medical Sciences (approval number: 2025B058), and met the requirements of the Beijing Administration Rule of Laboratory Animals.

Male C57BL/6J mice (20–25 g) were housed under standard conditions with a 12-hour light-dark cycle and provided *ad libitum* access to food and water. Anesthesia was induced and maintained by continuous isoflurane inhalation. Mice were positioned in dorsal recumbency, and a midline cervical incision was made to expose the carotid arteries. The external carotid artery (ECA), right common carotid artery (CCA), and internal carotid artery (ICA) were carefully dissected and ligated. A nylon monofilament (0.20 ± 0.01 mm) was inserted into the ICA through the CCA until reaching the origin of the middle cerebral artery. After 30 minutes of occlusion, the filament was withdrawn to allow for reperfusion, followed by permanent ligation of the CCA. Sham-operated mice underwent identical surgical procedures, without filament insertion or vascular occlusion. Ori (10, 20, and 40 mg/kg) or an equivalent volume of normal saline (vehicle control) was injected intraperitoneally (i.p.) 24 hours before surgery and 5 minutes before reperfusion, based on a previous study, with minor modifications[17].

Half-maximal inhibitory concentration determination and OGD/R model

The half-maximal inhibitory concentrations (IC_{50}s) of Ori and Ori-p were evaluated in Neuro-2a cells and primary cortical neurons. Neuro-2a cells were cultured to 90% confluence, enzymatically dissociated, and seeded in 96-well plates at 3×10^5 cells/mL. After 24 hours of adhesion, cells were exposed to graded concentrations of Ori or Ori-p for an additional 24 hours. Primary neuronal cultures were plated directly in 96-well plates and allowed to mature for 7 days *in vitro* prior to treatment with the test compounds at varying concentrations for 24 hours. Cell viability was quantitatively assessed using the CCK-8 assay.

The OGD/R model was established as previously described[18]. Neuro-2a cells were seeded in 96- or 6-well plates at 3×10^5 cells/mL and divided into three experimental groups: Control, OGD/R, and OGD/R + Ori. After 12 hours of incubation, the control and OGD/R groups received 0.1% DMSO, while the OGD/R + Ori group was treated with Ori for 24 hours. Both OGD/R and OGD/R + Ori groups were then subjected to oxygen-glucose deprivation (OGD) by replacing the medium with glucose-free DMEM and incubating in a hypoxic chamber (95% N_2/5% CO_2) for 4 hours, followed by reperfusion with complete DMEM for 24 hours. Cell viability was assessed using the CCK-8 assay in 96-well plates, while cells from six-well plates were collected for further analysis. Primary neurons cultured for 7 days underwent identical treatments.

Neurological assessment and brain tissue analysis

Neurological deficits were evaluated 24 hours post-transient middle cerebral artery occlusion (tMCAO) using the Zea-Longa scoring system (0–5 scale) by a blinded investigator, and higher scores indicated more severe impairment[18]. For infarct volume quantification, brains were rapidly extracted and flash-frozen at –80°C for 5 minutes and coronally sectioned into six 2-mm slices using a brain matrix. Sections were stained with 1% TTC at 37°C for 15 minutes, followed by overnight fixation in 4% paraformaldehyde (PFA). Infarct volume was calculated using ImageJ software. For histological evaluation, brains were fixed in 4% PFA, paraffin-embedded, and sectioned at 4-μm thickness for hematoxylin and eosin (H&E) staining. For immunofluorescence (IF), mice were transcardially perfused with PBS followed by 4% PFA, and then the brains were cryoprotected in Tissue-Tek® O.C.T. compound and cryosectioned at 7 μm thickness.

Proteome-wide reactivity profiling of Ori-p

Neuro-2a cell lysates (150 μg per group) were incubated with increasing concentrations of Ori-p (0, 1.25, 2.5,

5, 10, 20 μM) for 4 hours, or with graded concentrations of Ori (20, 40, 60, 80 μM) for 1 hour followed by 20 μM Ori-p for 4 hours. Following labeling, samples underwent copper-catalyzed click chemistry conjugation (reagent details in reference[18]) for 2 hours at 25°C. Proteins were acetone-precipitated at –20°C for 1 hour, pelleted by centrifugation, and resuspended in loading buffer *via* ultrasonication. Samples were boiled at 95°C for 5 minutes, separated by SDS-PAGE, and visualized using in-gel fluorescence scanning. Total protein profiles were assessed using Coomassie brilliant blue (CBB) staining (10 minutes) and appropriate destaining.

Target identification of Ori via pull-down and WB

For target identification, Neuro-2a cell lysates (2 mg per group) were divided into control (0.1% DMSO), Ori-p (20 μM), and compete (Ori-p, 20 μM + Ori, 80 μM) groups. The compete group received Ori pretreatment for 1 hour prior to Ori-p incubation for 4 hours. Click chemistry conjugation was performed for 2 hours as previously described[18]. Proteins were precipitated with ice-cold acetone at –20°C for 1 hour, pelleted by centrifugation, and solubilized in 600 μL 1.5% SDS by ultrasonication. Samples were boiled at 95°C for 10 minutes, then diluted to 0.1% SDS with PBS, and centrifuged to remove highly denatured proteins. The supernatant was incubated with streptavidin beads for 4 to 6 hours with rotation at 25°C. Beads were washed sequentially with SDS and urea buffers to remove nonspecifically bound proteins. The bound proteins were reduced with 5 mM dithiothreitol (DTT, 30 minutes) and alkylated with 25 mM iodoacetamide (IAA, 45 minutes in the dark). Sequencing-grade modified trypsin was used to hydrolyze proteins into peptides at 37°C for over 16 hours. Peptides were desalted, labeled with TMT reagents (127N: control, 131: Ori-p, and 129N: compete) at 37°C for 2 hours, protected from light, and desalted again prior to LC-MS/MS analysis. Proteins with enrichment ratios $R_{(Ori\text{-}p/Compete)}$ >1.2 and $P < 0.05$ were considered high-reliability targets. For validation, Neuro-2a and primary neuron lysates (2 mg per group) were processed similarly, and streptavidin bead-enriched proteins were analyzed by WB to verify HMGB1 labeling by Ori-p.

Cellular thermal shift assay/WB analysis

Cellular thermal shift assay (CETSA) was performed using Neuro-2a cell lysates (2 mg per group) divided into control (0.1% DMSO) and Ori-treated (10 μM) groups. Following 1 hour incubation at 25°C, each treatment group was aliquoted into 10 equal portions for temperature gradient analysis. After thermal treatment, samples were centrifuged to separate soluble proteins. Equal volumes of supernatant from each temperature point were mixed with loading buffer, denatured at 95°C for 10 minutes, and analyzed by SDS-PAGE and WB to assess the thermal stability profiles of target proteins.

IF staining

Neuro-2a cells were plated in confocal imaging chambers and treated with 20 μM Ori-p for varying durations, or pretreated with Ori for 4 hours followed by Ori-p exposure. Following treatment, the cells were sequentially processed as follows: washed with PBS (twice, 5 minutes each), fixed with 4% PFA (10 minutes), permeabilized with 0.2% Triton X-100 (15 minutes), and blocked with 5% BSA (1 hour). Primary antibody incubation with anti-HMGB1 (1:100) was performed overnight at 4°C. After primary antibody incubation, click chemistry conjugation was performed for 2 hours at 25°C. Cells were then incubated with fluorophore-conjugated secondary antibody (1:500, 1 hour), followed by three TBST washes (5 minutes each). Nuclei were counterstained with Hoechst 33342 containing antifade mounting medium prior to confocal microscopy using appropriate filter sets for each fluorophore.

HMGB1 protein labeling

To investigate the interaction between Ori and HMGB1, recombinant human HMGB1 B-box and HMGB1-Cys106 mutants (Cys106 replaced with glycine) were prepared as previously described[19]. For binding characterization, various concentrations of Ori with 2 μg HMGB1 or varying HMGB1 concentrations (0, 2, 3, or 4 μg) with 10 μM Ori were labeled separately. Competitive labeling experiments were performed using 2 μg HMGB1 per group, where the cysteine-reactive agent IAA (10×) or alkynyl-IAA probe (IAA-yne, 10 μM) was introduced to compete with Ori-p (10 μM) or Ori (10×) to validate cysteine-dependent binding. To further assess binding specificity, hydrogenated Ori (H-Ori, 5× or 10×) was tested against HMGB1 (2 μg per group) pretreated with Ori-p (10 μM) and IAA-yne (10 μM). Additionally, wild-type HMGB1 (2 μg per group) and the HMGB1-Cys106 mutant (H-Cys106, 2 μg per group) were incubated with increasing concentrations of Ori-p (10 μM for HMGB1; 5, 10, or 20 μM for H-Cys106). Following click chemistry conjugation, samples were mixed with loading buffer, separated by SDS-PAGE, and visualized using a laser imaging system. Total protein profiles were confirmed with CBB staining and destaining.

Molecular docking and biolayer interferometry

Binding interactions between Ori and HMGB1 (or its B-box domain) were investigated using computational and biophysical approaches. For molecular docking simulations, AutoDock 4.2.6 was employed. The structure of Ori was retrieved from PubChem (CID: 5321010), whereas the 3D structures of full-length HMGB1 and its B-box domain (amino acids 95–163) were predicted using AlphaFold3. Prior to molecular docking, protein and chemical structures were hydrogenated and dehydrated using AutoDock Tools, followed by flexible docking with default parameters. PyMOL software (version 2.5) was used to analyze and visualize intermolecular interactions.

Binding affinities between Ori and HMGB1 were quantitatively analyzed using biolayer interferometry (BLI, Sartorius). Purified human HMGB1 protein (30 μg) was immobilized onto streptavidin-coated biosensor tips, and serial dilutions of Ori (0–100 μM) were added. Binding kinetics were analyzed using Octet data analysis

software with a 1:1 binding model, and the equilibrium dissociation constant (Kd) was determined by global fitting.

Effect of Ori on HMGB1 and B-box activity

The effects of Ori on HMGB1 and its B-box domain were assessed in RAW 264.7 macrophages. Following trypsinization and centrifugation, cells were plated in 24-well plates and divided into experimental groups: (1) Untreated Control, (2) H-Cys106 mutant (1 μg), (3) HMGB1 (1 μg), and (4) HMGB1 (1 μg) co-treated with Ori (2 or 4 μg). After 24 hours of incubation, culture supernatants were collected for TNF-α quantification using an ELISA kit.

For B-box domain studies, recombinant B-box protein (50 μg) was preincubated with Ori (0 or 5 nM) for 1 hour at 25°C. Protein complexes were affinity-purified using Ni-NTA columns (4°C, 2 hours), eluted with 250 mM imidazole, and quantified using BCA assay. Functionally active fractions (0.02 and 0.20 μg) were applied to RAW 264.7 cultures, and TNF-α secretion was measured after 24 hours as described earlier.

Binding interactions between the HMGB1 B-box domain and its receptors (TLR4 and RAGE) were evaluated using the following procedure: Three experimental groups containing 100 μg recombinant B-box protein were prepared: (1) B-box alone (control), (2) B-box + 20 nM Ori, and (3) B-box + 40 nM Ori. Following 1 hour incubation at 25°C, each group was mixed with 500 μg of Neuro-2a cell lysate and loaded onto Ni-NTA affinity columns for binding at 4°C (2 hours). After washing with 250 mM imidazole, eluates were quantified by BCA assay, mixed with 5× loading buffer, and denatured prior to separation by 12% SDS-PAGE.

Quantification of HMGB1 secretion in cell culture supernatant

Neuro-2a cells and primary cortical neurons were divided into Model and Model + Ori groups. Following OGD/R induction with or without Ori (2 μM) treatment, supernatants were collected at 4, 8, and 24 hours post-reperfusion. The samples were centrifuged at 1,000× g for 10 minutes at 4°C to remove cellular debris. For each sample, 4 mL of the supernatant was filtered using a 50-kDa ultrafiltration tube to eliminate high-molecular-weight contaminants, followed by concentration (20×) using a 10-kDa ultrafiltration tube. Concentrated samples were then mixed with loading buffer, boiled, and subjected to WB analysis.

WB analysis

For cellular protein analysis, Neuro-2a cells and primary neurons were plated in 6-well plates (3×10^5 cells/mL) and subjected to OGD/R. At 24 hours post-treatment, cells were lysed, and protein concentrations were determined using a BCA protein assay kit. Brain tissue samples were collected from the right cerebral cortex of experimental mice following microdissection. All protein samples were denatured in 5× loading buffer at 95°C for 5 minutes. Nuclear and cytoplasmic extraction and separation kits were used to obtain cytoplasmic proteins from Neuro-2a cells, primary neurons, and mice cortex. WB was used to detect protein expression levels as described previously[20]. Proteins were separated by 8% to 13% SDS-PAGE and transferred to polyvinylidene fluoride membranes and blocked with 5% BSA in TBST for 1 hour before incubation with primary antibodies overnight at 4°C. Membranes were then washed with TBST and incubated with appropriate HRP-conjugated secondary antibodies for 1 hour, washed again, and visualized using a fluorescence WB imaging system. Band intensity was analyzed with ImageJ software.

NecroX-7

NecroX-7, an HMGB1 inhibitor, exerts protective effects by inhibiting HMGB1 release during I/R injury[21]. *In vitro*, cells were treated with NecroX-7 in the presence or absence of Ori (2 μM) for 24 hours, followed by OGD/R induction. Cell viability was assessed using the CCK-8 assay, and cell lysates were collected 24 hours later for WB analysis of TLR4, MyD88, and p-p65/p65 expression.

In vivo, NecroX-7 (1 mg/kg) was administered intraperitoneally 24 hours before surgery and 5 minutes before reperfusion, based on previous literature with modifications[22]. In the NecroX-7 + Ori group, NecroX-7 and Ori (20 mg/kg) were coadministered using the same regimen.

Statistical analysis

Statistical analysis was performed using GraphPad Prism 10.0, with data presented as mean ± standard error of the mean (SEM). One-way analysis of variance (ANOVA) was used for group comparisons. WB bands were quantified using ImageJ software. Differences between the two groups were tested using Fisher's least significant difference *post hoc* test. P value <0.05 was considered statistically significant.

Results

Ori treatment significantly reduced cerebral infarct volume and improved neurological function in tMCAO model mice

Figure 1A shows the animal experiment design. Compared with the Model group, Ori administration led to a dose-dependent reduction in infarct size (Figure 1B) and a marked improvement in neurological deficits, with the 20 mg/kg dose showing optimal neuroprotective efficacy (Figure 1C). Histopathological evaluation using H&E staining revealed that the Model group displayed severe neuronal damage in the cerebral cortex region, characterized by pyknotic nuclei, cytoplasmic vacuolation of varying sizes, inflammatory cell infiltration, and heterogeneous cytoplasmic staining. These pathological changes were markedly attenuated by Ori treatment, particularly at 20 mg/kg (Figure 1D).

Both Ori and Ori-p exhibited comparable neuroprotective effects in vitro

To explore the pharmacological targets of Ori, Ori-p was synthesized (Figure 2A). The cytotoxicity of both compounds was evaluated in Neuro-2a cells and primary

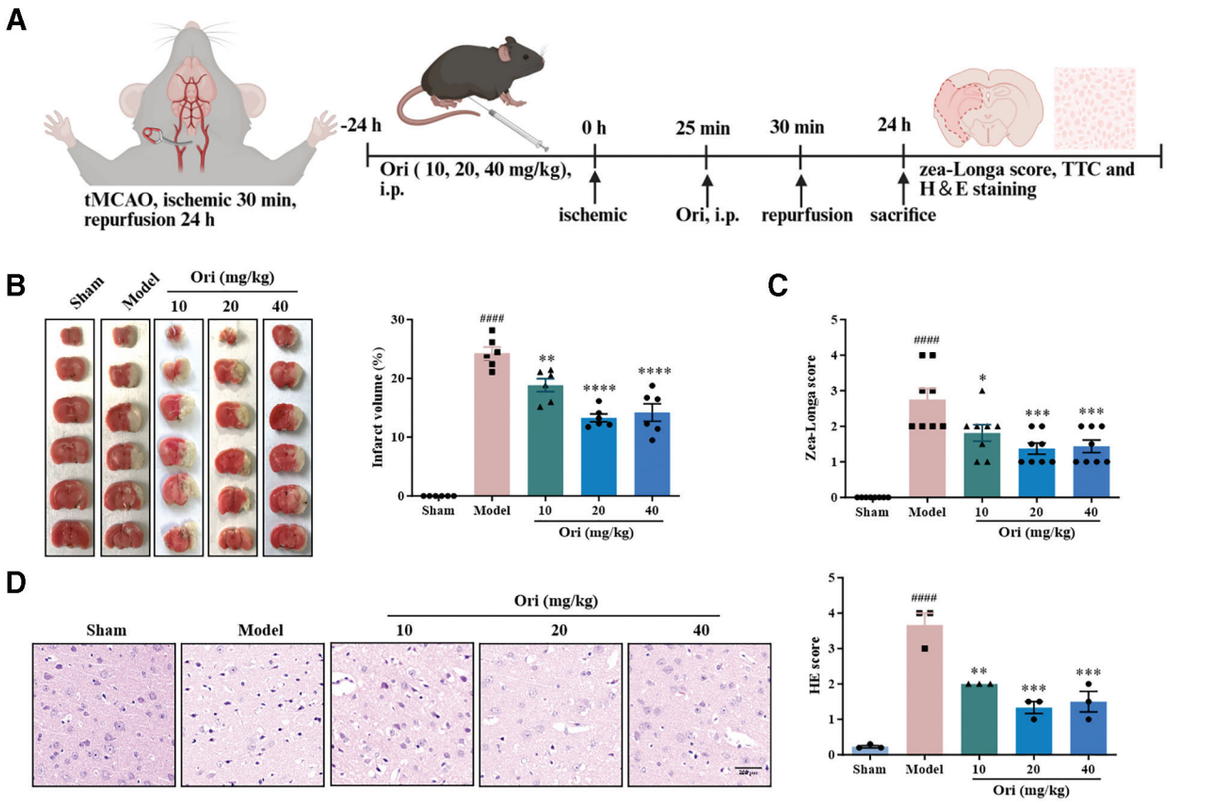

Figure 1. Ori attenuated cerebral I/R injury in mice. (A) Schematic timeline of animal experimental procedures. (B) Representative TTC-stained brain sections and quantitative analysis of infarct volume at 24 h post-tMCAO (n = 6). (C) Neurological function assessed by modified Zea-Longa scores (n = 8). (D) Histopathological evaluation *via* H&E staining (scale bar = 200 μm) and semiquantitative damage scoring (n = 3). Data were presented as mean ± SEM. $^{####}P < 0.0001$ *vs.* sham group, $^{**}P < 0.01$ vs. model group $^{***}P < 0.001$ *vs.* model group (one-way ANOVA with *post hoc* analysis). ANOVA: analysis of variance; H&E: Hematoxylin and eosin; I/R: Ischemic–reperfusion; SEM: Standard error of the mean; tMCAO: Transient middle cerebral artery occlusion: TTC: 2,3,5-Triphenyltetrazolium chloride.

neurons after 24 hours. Concentration–response analysis revealed an IC_{50} of 14.28 μM for Ori *versus* 7.65 μM for Ori-p in Neuro-2a cells (Figure 2B), whereas in primary neurons, IC_{50} values were 18.17 and 15.71 μM, respectively (Figure 2C). Both compounds exhibited concentration-dependent cytotoxicity. The similar IC_{50} profiles indicated that Ori-p retained pharmacological properties comparable to those of the parent Ori molecule, confirming that Ori preserved its biological activity after the introduction of a bioorthogonal reactive group.

Based on IC_{50} determinations, a concentration range of 0.5 to 10 μM Ori was selected for subsequent experiments to evaluate its neuroprotective efficacy. After 24 hours of pretreatment with various Ori concentrations, cells were subjected to OGD/R injury, and cell viability was assessed using the CCK-8 assay after an additional 24 hours. Ori (0.5–4 μM) exerted significant neuroprotective effects against OGD/R injury in both Neuro-2a cells (Figure 2D) and primary neurons (Figure 2E). Extending these findings to the modified compound, parallel experiments demonstrated that Ori-p similarly exhibited pronounced neuroprotection in Neuro-2a cells (Figure 2F) and primary neurons (Figure 2G). These results not only validated the preservation of Ori's original pharmacological activity in its derivative Ori-p but also confirmed that the structural modifications introduced for bioorthogonal reactions did not compromise its neuroprotective properties.

Ori reduced inflammatory factor expression following OGD/R and tMCAO

Given the critical role of neuroinflammation in cerebral I/R injury development and prior reports of Ori's anti-inflammatory properties in other disease models[14], we systematically analyzed the expression of inflammatory mediators by WB. Comparative analysis revealed substantial upregulation of IL-1β, IL-6, COX-2, and iNOS protein levels in both the vehicle-treated OGD/R model of Neuro-2a cells (Figure 3A), primary neurons (Figure 3B), and tMCAO mice (Figure 3C) when compared with those in the control group or sham-operated mice. Notably, Ori treatment effectively reversed these inflammatory responses, consistently demonstrating potent anti-inflammatory activity in both neuronal cell models and the mouse cerebral ischemic model, thereby confirming its therapeutic potential against I/R-induced neuroinflammation.

Ori-p exhibited high bioconjugation efficiency and target recognition

Neuro-2a cell lysates were collected for *in vitro* protein-labeling experiments to investigate the labeling efficiency of Ori-p. As shown in Figure 4A, fluorescent labeling assays revealed a concentration-dependent increase in fluorescent signal, with 20 μM Ori-p achieving optimal labeling efficiency. Competitive binding experiments

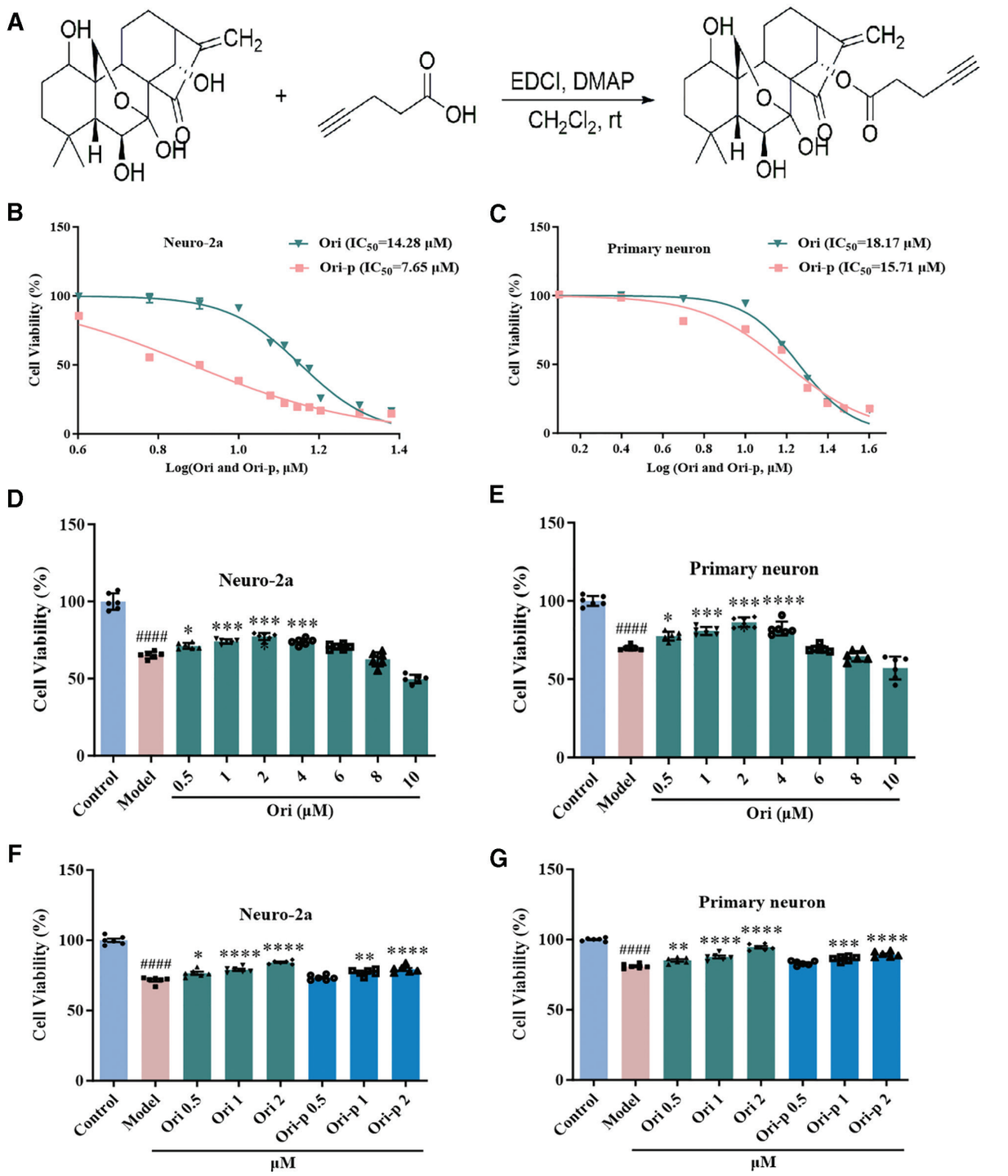

Figure 2. Pharmacological characterization of Ori-p demonstrated conserved bioactivity relative to parent compound Ori. (A) Synthetic scheme for the preparation of Ori-p. (B, C) Concentration–response curves and calculated IC_{50} values for Ori and Ori-p in Neuro-2a cells (B) and primary neurons (C) (n = 6). (D, E) Neuroprotective effects of Ori pretreatment against OGD/R-induced injury in Neuro-2a cells (D) and primary neurons (E) (n = 6). (F, G) Comparative neuroprotection by Ori and Ori-p in OGD/R models using Neuro-2a cells (F) and primary neurons (G) (n = 6). Data were presented as mean ± SEM. $^{\#\#\#\#}P < 0.0001$ *vs.* control group, $^{*}P < 0.05$, $^{**}P < 0.01$, $^{***}P < 0.001$, $^{****}P < 0.0001$ *vs.* model group (one-way ANOVA with *post hoc* analysis). ANOVA: analysis of variance; DMAP: 4-dimethylaminopyridine; EDCI: 1-ethyl-3-(3-dimethylaminopropyl)carbodiimide; IC_{50}: Half-maximal inhibitory concentration; OGD/R: Oxygen-glucose deprivation/reperfusion; Ori-p: Oridonin-probe; SEM: Standard error of the mean.

further confirmed the target specificity. Pretreatment of lysates with increasing concentrations of Ori for 1 hour prior to 20 μM Ori-p incubation for 4 hours resulted in a dose-dependent reduction in fluorescence intensity (Figure 4B). This competitive inhibition pattern strongly suggests that Ori-p shares binding targets with the parent Ori compound.

Comprehensive proteomic analysis identified potential molecular targets of Ori. Venn diagram analysis of pull-down assay results revealed 138 high-confidence

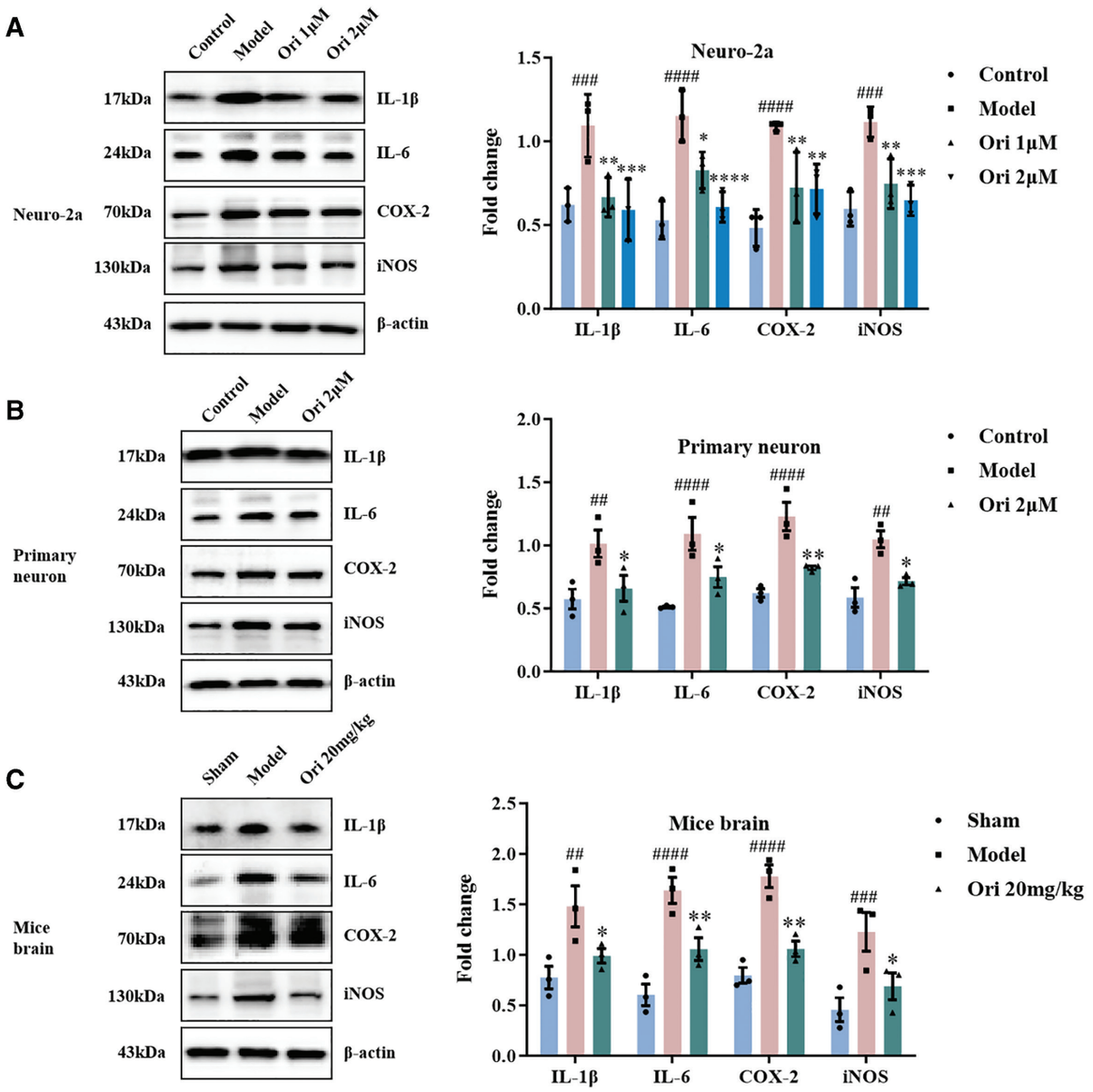

Figure 3. Ori attenuated neuroinflammation in cerebral I/R injury models. (A) WB analysis and quantitative densitometry of pro-inflammatory mediators (IL-1β, IL-6, COX-2, iNOS) in OGD/R-challenged Neuro-2a cells, normalized to control ($n = 3$). (B) Corresponding inflammatory protein expression profiles in primary neurons post-OGD/R ($n = 3$). (C) Cortical expression of inflammatory markers 24 h post-tMCAO in mice, with sham-operated animals as reference ($n = 3$). Data were presented as mean ± SEM. $^{\#\#}P < 0.01$, $^{\#\#\#}P < 0.001$, $^{\#\#\#\#}P < 0.0001$ *vs.* control/sham group, $^{*}P < 0.05$, $^{**}P < 0.01$, $^{***}P < 0.001$, $^{****}P < 0.0001$ *vs.* model group (one-way ANOVA with *post hoc* analysis). ANOVA: Analysis of variance; COX: Cyclooxygenase; I/R: Ischemic–reperfusion; IL: Interleukin; iNOS: Inducible nitric oxide synthase; OGD/R: Oxygen-glucose deprivation/reperfusion; Ori: Oridonin; SEM: Standard error of the mean; tMCAO: Transient middle cerebral artery occlusion; WB: Western blot.

protein targets that specifically interacted with Ori, after eliminating false-positives (Figure 4C). A total of 148, 142, and 14 differentially expressed proteins were identified in the Ori-p *versus* control, compete *versus* control, and compete *versus* Ori-p groups, respectively (Figure 4D). Kyoto Encyclopedia of Genes and Genomes (KEGG) pathway analysis showed that the 138 Ori targets were significantly enriched in critical signaling pathways, particularly the Toll-like receptor and AGE/RAGE signaling pathways (Figure 4E). Heatmap analysis highlighted 14 high-confidence targets that showed complete competition with Ori (Figure 4F). Cross-referencing with known IS targets from GeneCards (https://www.genecards.org/) identified seven overlapping therapeutic targets, most notably, HMGB1 (Figure 4G). Multiple lines of evidence indicated HMGB1 as a primary target of Ori: (1) it ranked first in high-confidence target heatmap; (2) competitive labeling assays showed near-complete displacement of 25-kDa proteins (matching HMGB1's molecular weight) by Ori treatment (Figure 4B, ★); (3) HMGB1 is functionally linked with both TLR4 and RAGE signaling cascades; and (4) HMGB1 plays a well-established role in IS pathogenesis. Collectively, these findings strongly support HMGB1 as a key molecular target mediating Ori's therapeutic effect against IS.

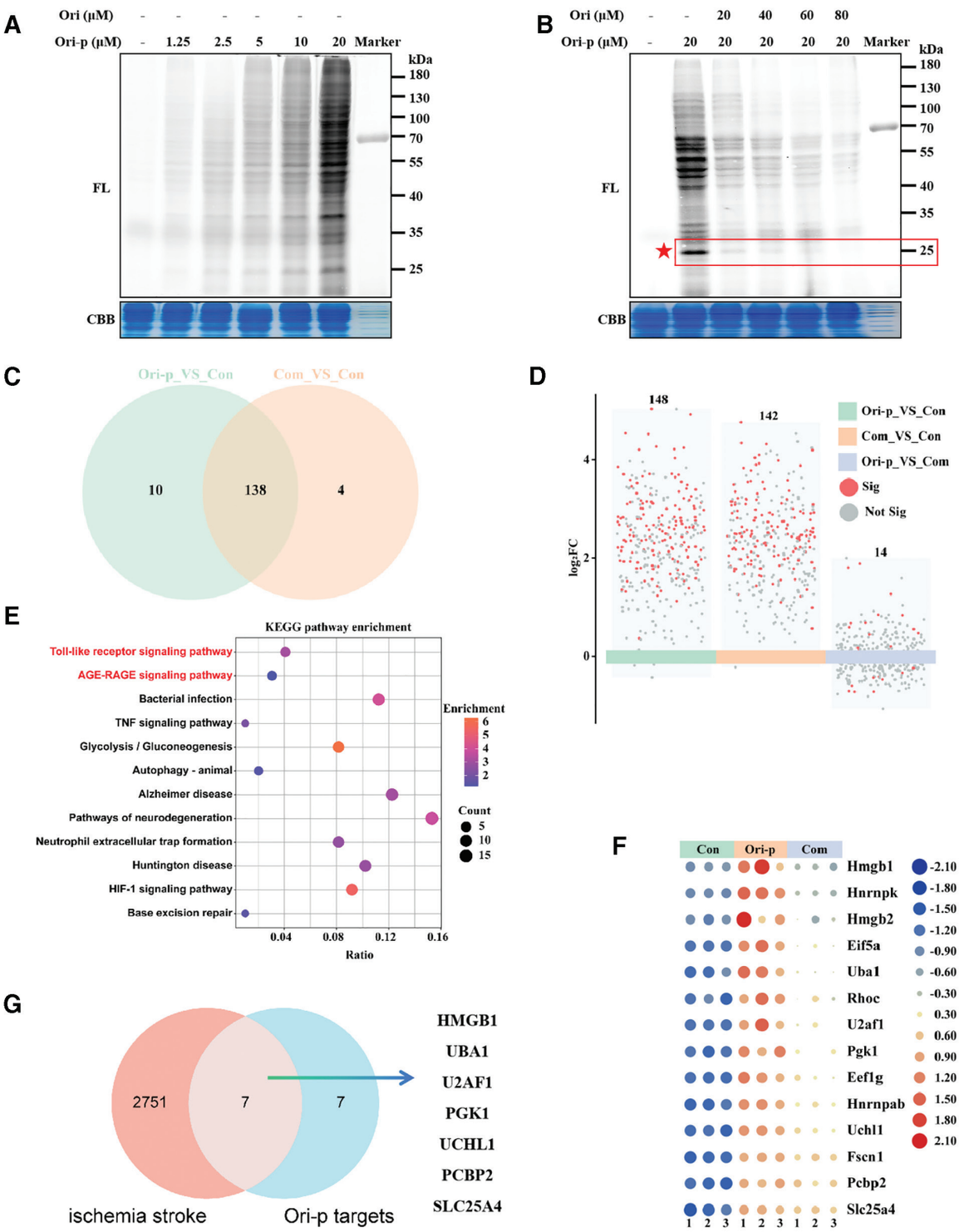

Figure 4. Chemoproteomic profiling identified HMGB1 as a key target of Ori in cerebral ischemic. (A) Dose-responsive fluorescent labeling of cellular proteins by Ori-p probe. (B) Competitive labeling profiles of Ori-p in the presence of Ori (1 ×, 2 ×, 3 ×, 4 ×). (C) Venn diagram displayed the number and overlap of proteins significantly enriched in pull-down assay of Ori. (D) Differentially expressed proteins across experimental groups were identified by quantitative proteomics (LC-MS/MS). (E) KEGG pathway enrichment of Ori targets highlighting TLR and AGE-RAGE signaling. (F) Heatmap of 14 high-affinity targets showing complete competition by Ori. (G) Target intersection analysis identifying 7 shared proteins between Ori targets and known IS mediators (GeneCards). AGE: Advanced glycation end products; CBB: Coomassie brilliant blue staining; FL: In-gel fluorescence; HIF: Hypoxia-inducible factor; HMGB1: High-mobility group box 1; IS: Ischemic stroke; KEGG: Kyoto Encyclopedia of Genes and Genomes; LC-MS/MS: Liquid chromatography-tandem mass spectrometry; Ori-p: Oridonin-probe; RAGE: Receptor for advanced glycation end products; TLR: Toll-like receptor; TNF: Tumor necrosis factor.

Interaction between Ori and HMGB1 was validated

Competitive pull-down/WB analysis demonstrated specific competition of Ori-p binding to HMGB1: pretreatment with Ori (4 ×, 80 μM) effectively abolished Ori-p (20 μM)-mediated HMGB1 labeling observed in control samples (Figure 5A). CETSA/WB analysis provided additional evidence for direct interaction, showing significant significantly greater thermal stabilization of HMGB1 in the presence of Ori (10 μM) across a broad temperature range (37°C–82°C) than untreated controls (Figure 5B). IF imaging further confirmed the specific interaction, revealing a time-dependent colocalization of Ori-p with HMGB1 within cellular compartments (Figure 5C). Together, these multimodal validations combining competitive binding, thermal stability profiling, and spatial localization provided conclusive evidence of a direct and specific molecular interaction between Ori and HMGB1.

Ori covalently bound to Cys106 of HMGB1 and diminished its proinflammatory activity

The α, β-unsaturated carbonyl group of Ori functions as an electrophilic Michael acceptor that selectively forms covalent bonds with nucleophilic cysteine sulfhydryl groups. To characterize this interaction with HMGB1, systematic binding assays were performed using recombinant human HMGB1 protein, which established: (1) bidirectional, dose-dependent binding between Ori-p and HMGB1 (Figure 6A); (2) complete reciprocal inhibition in competitive binding assays with the cysteine-specific probe IAA-yne, where IAA abolished Ori-p-HMGB1 binding and vice versa (Figure 6B), confirming cysteine-dependent binding; (3) loss of binding capacity upon hydrogenation of Ori's critical carbon–carbon double bond (H-Ori, Figure 6C).

HMGB1 comprises three structural domains:the A-box, the B-box, and an acidic tail. When Cys23/Cys45 in the A-box form disulfide bonds and Cys106 in the B-box remains free, HMGB1 exhibits proinflammatory activity[23]. To determine whether Cys 106 was responsible for Ori binding, an HMGB1 mutant in which Cys106 was changed to glycine was constructed. Figure 6D shows that the mutation abolished the Ori-p binding. Molecular docking simulations revealed strong spatial complementarity between Ori and HMGB1 or its B-box, with a particular affinity for Cys106 (Figure 6E). BLI quantified this interaction and demonstrated specific binding with a Kd value of 26.41 μM (Figure 6F). Collectively, these multidisciplinary results identified Cys106 as the key residue responsible for covalent modification by Ori.

Structural and functional studies have established that HMGB1's proinflammatory properties primarily reside in its B-box domain, whereas the A-box domain antagonizes inflammation[24]. Our findings demonstrated that Ori specifically targets Cys106 in the B-box. To elucidate the functional consequences of this interaction, we examined Ori's modulation of HMGB1 or B-box-induced TNF-α secretion in RAW264.7 macrophages, following established methodologies[18]. As shown in Figure 6G, wild-type HMGB1 robustly

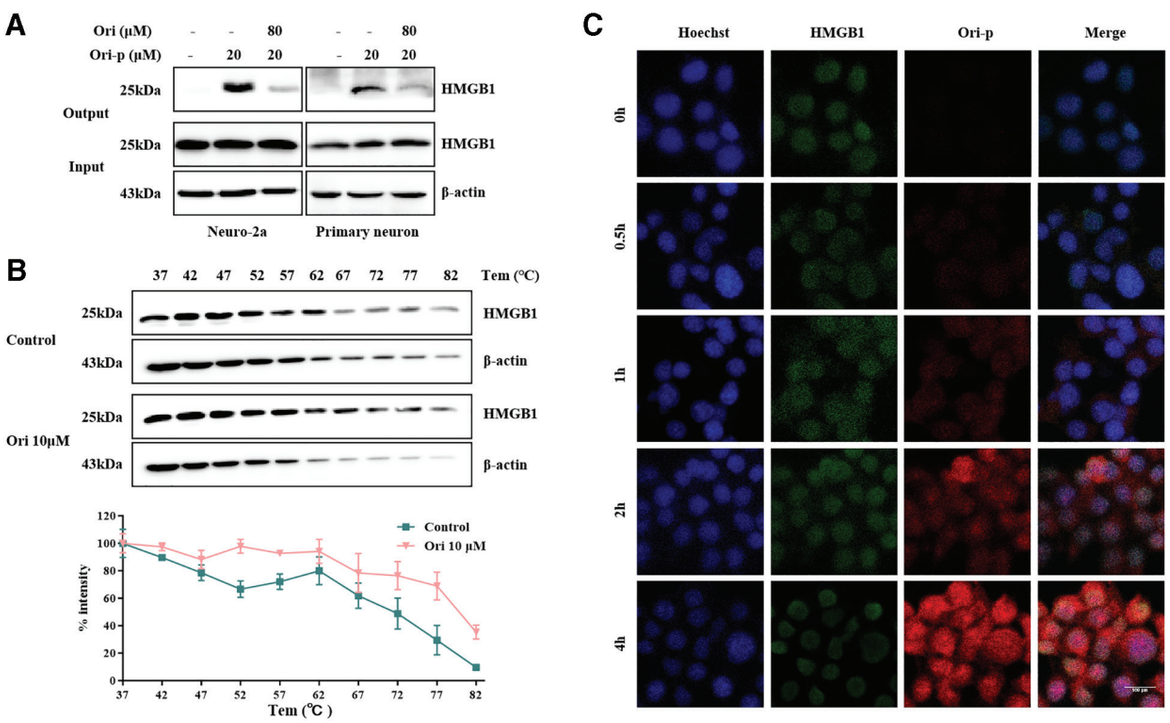

Figure 5. Direct binding interaction between Ori and HMGB1. (A) Competitive pull-down/WB analysis verified that Ori 4× completely competed away the binding of Ori-p to HMGB1 in both Neuro-2a cells and primary neurons. (B) CETSA/WB confirming HMGB1 thermal stabilization upon Ori treatment in Neuro-2a lysates (n = 3). (C) IF visualization of time-dependent co-localization between HMGB1 (green) and Ori-p (red) in Neuro-2a cells (200×; scale bar = 100 μm). CETSA: Cellular Thermal Shift Assay; HMGB1: High-mobility group box 1; Ori-p: Oridonin-probe; WB: Western blot.

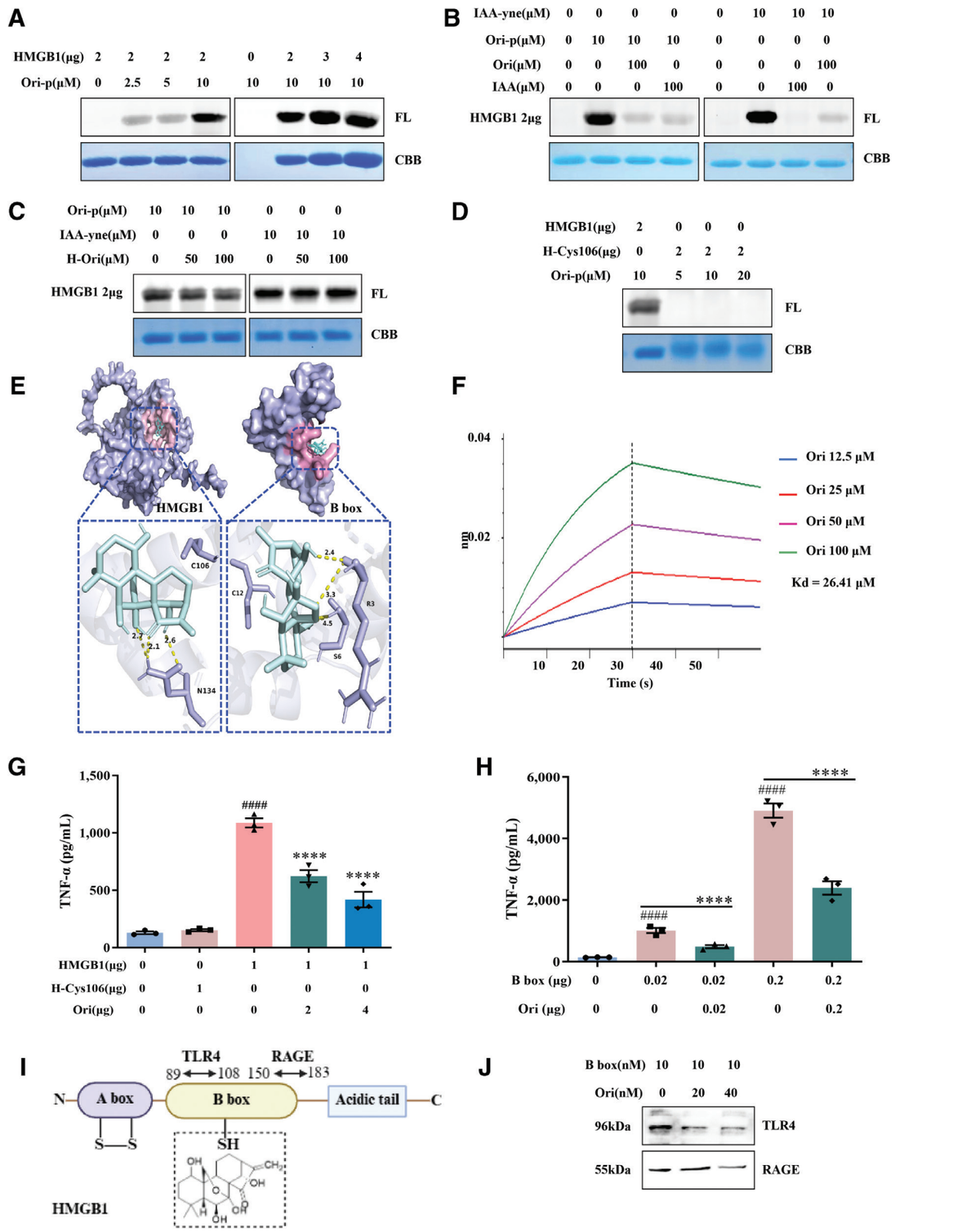

Figure 6. Structural and functional characterization of Ori covalent modification of HMGB1 at Cys106. (A) Concentration-dependent binding between Ori-p and recombinant HMGB1 protein. (B) Reciprocal competition assays. IAA almost entirely competed away the binding of Ori-p with HMGB1, and Ori near-complete inhibition of IAA-yne with HMGB1, confirming cysteine-dependent interaction. (C) Loss of competitive binding capacity with HMGB1 upon hydrogenation of Ori's critical α, β-unsaturated carbonyl (H-Ori). (D) Abolished binding to Cys106-HMGB1 mutant, establishing Cys106 as the essential modification site. (E) Molecular docking revealing spatial alignment between Ori and HMGB1/B box analyzed with Trips molecular modeling software. (F) BLI for the binding affinity between Ori and HMGB1. (G, H) Significant suppression of HMGB1/B box-induced TNF-α secretion by Ori treatment in RAW264.7 cells (n = 6). (I) Schematic of Ori's binding site (Cys106) relative to TLR4/RAGE interaction domains on HMGB1. (J) Representative WB for TLR4 and RAGE in total cell lysates of Neuro-2a cells. Data were presented as mean ± SEM. ####P < 0.0001 *vs.* control group, ****P < 0.0001 *vs.* HMGB1/B box group (one-way ANOVA with *post hoc* analysis). ANOVA: Analysis of variance; BLI: Biolayer interferometry; H-Ori: Hydrogenated Oridonin; HMGB1: High-mobility group box 1; IAA: Iodoacetamide; Ori-p: Oridonin-probe; RAGE: Receptor for advanced glycation end products; SEM: Standard error of the mean; TLR: Toll-like receptor; TNF: Tumor necrosis factor.

stimulated TNF-α production, whereas the Cys106 mutant exhibited a loss of proinflammatory activity. Furthermore, the combination of Ori and HMGB1 weakened the proinflammatory effects. The B-box significantly induced TNF-α release, which was markedly suppressed by Ori co-treatment (Figure 6H). The anti-inflammatory mechanisms were investigated using receptor interaction studies. Previous reports have identified two critical HMGB1 receptors: TLR4 (binding to B-box residues 89-108) and RAGE (binding to residues 150–183)[25]. Our results demonstrated that Ori covalent modification of Cys106 in the B-box domain sterically interfered with both TLR4 and RAGE binding (Figure 6I, J), providing a structural basis for its anti-inflammatory effects. Collectively, these findings established that Ori exerts its anti-inflammatory activity primarily through the carbon–carbon double bond-mediated covalent modification of Cys106 in HMGB1's B-box domain, thereby disrupting its interaction with the proinflammatory receptors TLR4 and RAGE.

Ori reduced the secretion of HMGB1 and suppressed the HMGB1/TLR4/MyD88/NF-κB signaling pathway

As a well-characterized DAMP, extracellular HMGB1 triggers inflammatory cascades through receptor binding[26], and clinical studies have demonstrated that elevated serum HMGB1 levels correlate with poor prognosis and increased recurrence of IS[27]. We detected the secretion of HMGB1 in the culture supernatant of cells using WB and ELISA and in the serum of mice using an ELISA kit. Our experimental data revealed that Ori treatment significantly reduced HMGB1 secretion after OGD/R in Neuro-2a cells and primary neurons (Figure 7A–C) and tMCAO injury in mice (Figure 7D).

Mechanistic studies further demonstrate that HMGB1-mediated inflammation occurs through TLR4 receptor activation and subsequent MyD88/NF-κB pathway stimulation[26]. Comprehensive analysis of this signaling cascade showed that Ori treatment effectively decreased cytoplasmic HMGB1 accumulation, downregulated TLR4 and MyD88 levels, and inhibited NF-κB activation (as measured by the p-p65/p65 ratio) in both OGD/R-treated neuronal cells (Neuro-2a: Figure 7E; primary neurons: Figure 7F) and tMCAO mouse brain tissues (Figure 7G). These consistent findings across *in vitro* and *in vivo* models established Ori as a potent modulator of the HMGB1-initiated inflammatory pathway, from DAMP release to downstream signaling events.

Ori exerted neuroprotective effects in cerebral I/R through HMGB1 dependence

To confirm whether Ori's neuroprotective effects were mediated through HMGB1, the HMGB1-specific pharmacological inhibitor NecroX-7 was used in both *in vitro* and *in vivo* cerebral I/R injury models. In cellular studies, NecroX-7 (20 μM) conferred significant neuroprotection in both OGD/R-challenged Neuro-2a cells and primary neurons, as evidenced by CCK-8 assay findings (Figure 8A) but showed no additive effects when combined with Ori (Figure 8B). WB analysis revealed that NecroX-7 alone effectively downregulated the key components of the HMGB1/TLR4/MyD88/NF-κB pathway (TLR4, MyD88, and p-p65/p65) in OGD/R-challenged Neuro-2a cells (Figure 8C) and primary neurons (Figure 8D). Notably, addition of Ori to NecroX-7-treated cells did not further reduce these inflammatory marker levels, suggesting a shared mechanism.

In vivo experiments corroborated these findings, with NecroX-7 administration significantly reducing the cerebral infarct volume (TTC staining, Figure 8E) and improving neurological deficits (Zea-Longa scores, Figure 8F) in tMCAO mice. In addition, combined NecroX-7 and Ori treatment failed to produce additional suppression of TLR4, MyD88, and p-p65/p65 expression in mice subjected to tMCAO (Figure 8G). These consistent observations across the experimental models demonstrate that the therapeutic actions of Ori occur primarily *via* HMGB1-dependent mechanisms. Collectively, our data established that Ori mediates its neuroprotection by specifically targeting HMGB1 and subsequently inhibiting the downstream HMGB1/TLR4/MyD88/NF-κB inflammatory signaling cascade.

Discussion

Donglingcao (*Rabdosia rubescens*) is a traditional Chinese medicinal herb containing multiple bioactive components, including Ori, volatile oils, Rubensensine B, and ursolic acid[12]. Ori was first isolated in the 1960s and has demonstrated diverse pharmacological activities, including anticancer, anti-inflammatory, immunomodulatory, and neuroprotective effects[28]. Accumulating evidence highlights the neuroprotective potential of Ori *via* the modulation of neuroinflammatory pathways[14]. By blocking the interaction between NLRP3 and NEK7, Ori inhibits neuroinflammation and autophagy impairment in chronic unpredictable mild stress-induced depression[29]. In cerebral amyloidosis for Alzheimer's disease, transgenic APP/PS1 mice, Ori effectively reduced inflammatory activation and ameliorated behavioral deficits[30]. In addition, Ori inhibited the neuroinflammation and activation of NF-κB, decreased mitochondrial injury, and improved cognitive impairment induced by $A\beta_{1\text{-}42}$[31]. Ori also ameliorates TBI-induced functional impairment and neurological damage by suppressing neuroinflammation and increasing antioxidant capacity and mitochondrial function by activating the Nrf2 pathway[32]. Our current findings further established Ori's therapeutic potential in cerebral I/R injury, demonstrating: (1) significant reduction of infarct volume and neurological deficits in tMCAO mice; (2) improved neuronal survival in OGD/R models; (3) potent anti-inflammatory effects through suppression of IL-1β, IL-6, COX-2, and iNOS expression. Prior studies on Ori have focused on the reperfusion phase, demonstrating its efficacy in inhibiting apoptosis to restore neuronal mitochondrial function when administered at the beginning of reperfusion[33]. Our novel addition of 24 hours pre-administration was designed to ensure the ability of Ori to attenuate ischemic brain injury. Both Ori treatments showed a comparable reduction in infarct volume, suggesting a

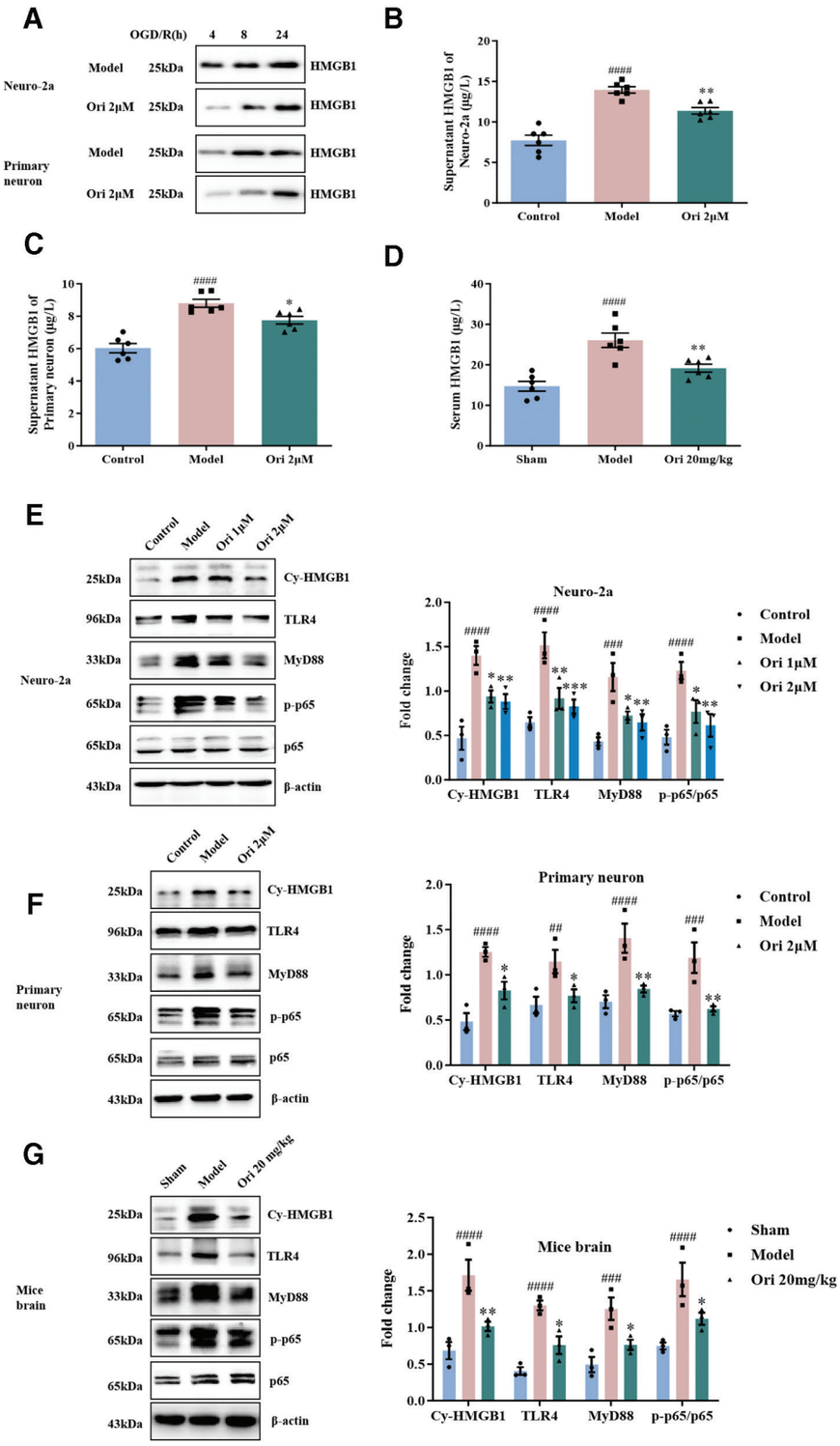

Figure 7. Ori inhibited HMGB1-mediated inflammatory signaling through multi-level regulation. (A) WB analysis of HMGB1 secretion in culture supernatants from OGD/R-challenged Neuro-2a cells and primary neurons. (B, C) Quantitative ELISA of extracellular HMGB1 in neuronal culture supernatants (Neuro-2a: B; primary neurons: C; $n = 6$). (D) Serum HMGB1 levels in tMCAO mice measured by ELISA ($n = 6$). (E) WB analysis of cytoplasmic HMGB1 translocation and downstream signaling mediators (MyD88, TLR4, p-p65/p65) in OGD/R-injured Neuro-2a cells, with densitometric quantification normalized to control ($n = 3$). (F) Corresponding pathway modulation in primary neurons post-OGD/R ($n = 3$). (G) Corresponding pathway modulation in mice cortex post-tMCAO, with sham-operated animals as reference ($n = 3$). Data are presented as mean ± SEM. $^{\#\#}P < 0.01$, $^{\#\#\#}P < 0.001$, $^{\#\#\#\#}P < 0.0001$ *vs.* control/sham group, $^{*}P < 0.05$, $^{**}P < 0.01$, $^{***}P < 0.001$ *vs.* model group (one-way ANOVA with *post hoc* analysis). ANOVA: Analysis of variance; ELISA: Enzyme-linked immunosorbent assay; HMGB1: High-mobility group box 1; OGD/R: Oxygen-glucose deprivation/reperfusion; Ori: Oridonin; SEM: Standard error of the mean; tMCAO: Transient middle cerebral artery occlusion; WB: Western blot.

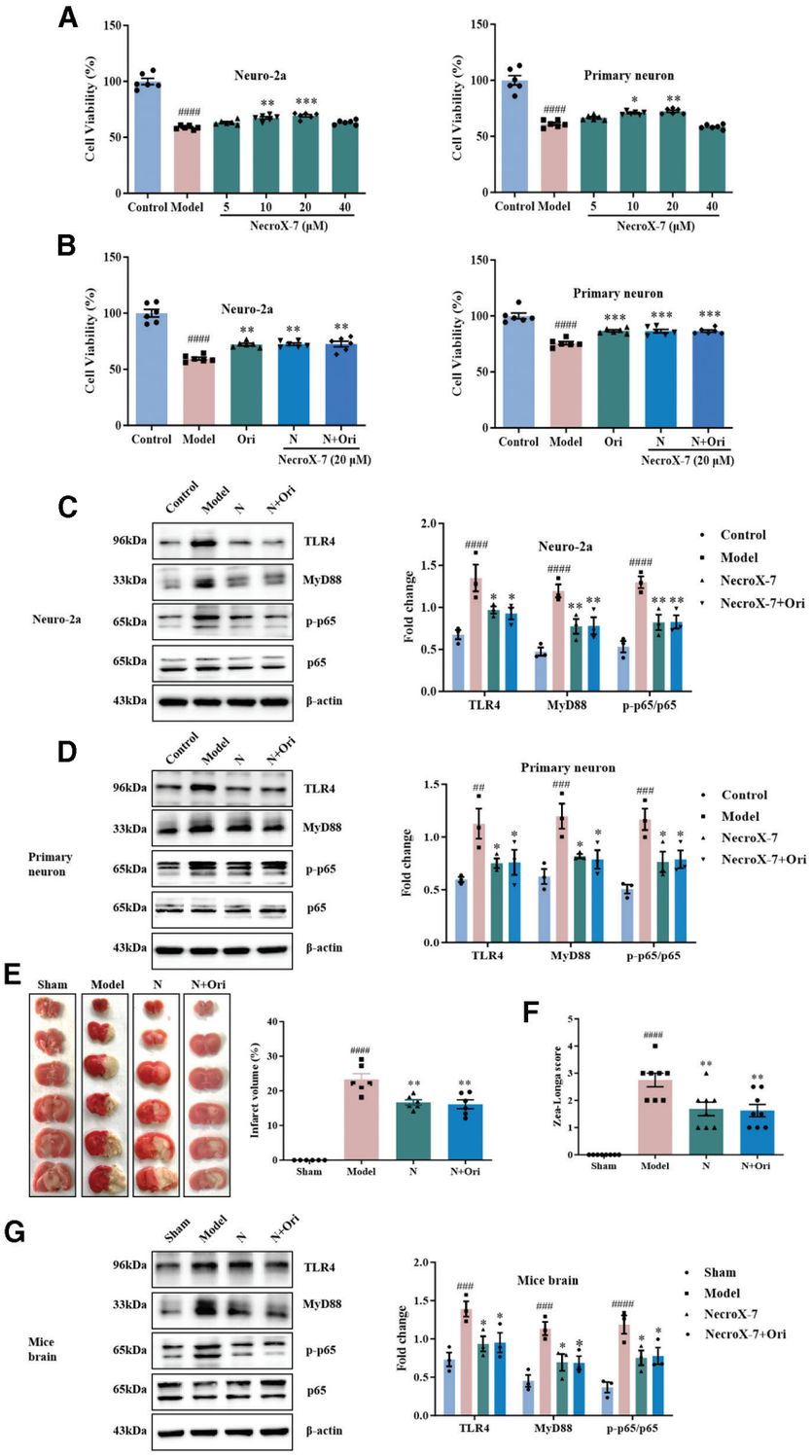

Figure 8. Pharmacological inhibition of HMGB1 by NecroX-7 replicated but did not potentiate Ori neuroprotection. (A) Concentration-dependent neuroprotection by NecroX-7 in OGD/R-injured Neuro-2a cells and primary neurons (CCK-8 assay, $n = 6$). (B) Absence of additive effects when combining NecroX-7 with Ori *in vitro* ($n = 6$). (C, D) WB analysis demonstrating NecroX-7-mediated downregulation of MyD88, TLR4, p-p65/p65 in (C) Neuro-2a cells and (D) primary neurons, with quantification normalized to control ($n = 3$). (E) Representative TTC-stained brain sections and quantitative analysis of infarct volume at 24 h post-tMCAO ($n = 6$). (F) Neurological function assessed by modified Zea-Longa scores ($n = 8$). (G) Cortical tissue analysis showing parallel pathway inhibition by NecroX-7 and Ori without combinatorial enhancement ($n = 3$). Data were presented as mean ± SEM. $^{###}P < 0.001$, $^{####}P < 0.0001$ *vs.* control/sham group, $^{*}P < 0.05$, $^{**}P < 0.01$, $^{***}P < 0.001$, $^{****}P < 0.0001$ *vs.* model group (one-way ANOVA with *post hoc* analysis). ANOVA: Analysis of variance; CCK-8: Cell counting kit-8; HMGB1: High-mobility group box 1; OGD/R: Oxygen-glucose deprivation/reperfusion; Ori: Oridonin; SEM: Standard error of the mean; tMCAO: Transient middle cerebral artery occlusion; TTC: 2,3,5-Triphenyltetrazolium chloride.

similar neuroprotective effect. Our pre-administration and pre-reperfusion treatment appeared effective at suppressing inflammatory responses (IL-1β, IL-6, COX-2, and iNOS) and inhibiting the HMGB1/TLR4/MyD88/NF-κB axis. Collectively, the accumulated evidence suggests that Ori is a multifaceted neuroprotective agent capable of targeting various pathological components of neurological disorders, with particular efficacy against neuroinflammation-mediated damage.

Through comprehensive characterization of the synthesized Ori-p and H-Ori derivatives, we systematically investigated the molecular targets and mechanisms underlying the therapeutic effects of Ori in cerebral I/R injury. Our target identification strategy prioritized HMGB1, a well-established mediator of neuroinflammation, based on its high-confidence interaction profile with Ori.

Structurally, HMGB1 is a non-histone nuclear protein characterized by two positively charged DNA-binding domains known as the A- and B-boxes, along with a negatively charged C-terminus (acidic tail)[23]. This nuclear protein exhibits remarkable functional pleiotropy, and its biological roles are dictated by its subcellular localization and redox state[34]. Under normal physiological conditions, HMGB1 mainly resides within the nucleus, where it maintains chromosomal structure and stability, while binding to DNA to participate in practically all DNA-dependent processes. However, cellular stress triggers its dynamic redistribution through passive release and active secretion into the cytoplasm and extracellular space, where it functions as a DAMP[35]. The inflammatory activity of extracellular HMGB1 is regulated by the redox state of its three cysteine residues (Cys23 and Cys45 in box A and Cys106 in box B). Notably, only the disulfide isoform (with a Cys23-Cys45 linkage and reduced Cys106) exhibits potent proinflammatory activity[36–37].

HMGB1 mediates its diverse effects by interacting with multiple cell surface receptors, including RAGE, TLR2/4/9, CXCL12, and various adhesion molecules, thereby enabling context-dependent signaling under different pathological conditions[23]. The TLR signaling pathway, in which extracellular HMGB1 acts as a DAMP that activates TLR2-/4-mediated inflammatory responses, is a critical mechanism in cerebral I/R injury. In the AGE-RAGE signaling pathway, the HMGB1–RAGE interaction exacerbates IS injury[34]. These additions strengthened HMGB1 as a primary target and provided a more robust foundation for downstream research. The proinflammatory activities of HMGB1 in response to sterile inflammation and infection are mainly mediated by the receptor TLR4 that activates the downstream signaling pathway, and TLR4 signaling is essential for HMGB1-mediated cytokine production[26,38]. In the context of brain injury, HMGB1 drives neuroinflammation predominantly through interactions with both TLR4 and RAGE receptors[25]. In our study, Ori markedly blocked the binding of TLR4 and RAGE to HMGB1's B-box domain, thereby reducing inflammatory activity. Clinically, elevated serum HMGB1 levels following cerebral ischemia correlate strongly with poorer outcomes and larger infarct volumes[39], while also serving as a potential biomarker for stroke-associated pneumonia in patients[40]. Mechanistically, we established that Ori significantly reduced HMGB1 secretion in both OGD/R and cerebral I/R injuries. Furthermore, Ori decreased cytoplasmic HMGB1 accumulation and potently inhibited the downstream HMGB1/TLR4/MyD88/NF-κB signaling cascade, collectively contributing to its anti-inflammatory and neuroprotective effects. These findings were further validated using the pharmacological inhibitor NecroX-7, which prevents HMGB1 release during I/R injury[41]. The parallel neuroprotective effects observed with both Ori and NecroX-7 treatments provide compelling evidence that HMGB1 serves as a primary molecular target mediating the therapeutic activity of Ori in cerebral I/R injury.

The inflammatory cascade during cerebral I/R involves distinct temporal patterns of HMGB1 release and modification. Initial HMGB1 release from necrotic neurons triggers early-phase neuroinflammation, whereas the subsequent redox modification of circulating HMGB1 activates peripheral immune responses[42]. Detailed characterization revealed that reduced HMGB1 was rapidly released within hours of ischemic onset, followed by the gradual accumulation of disulfide HMGB1 beginning 24 hours post-infarction[43]. Therapeutic interventions targeting HMGB1, including A-box administration and neutralizing antibodies, have demonstrated significant neuroprotective effects in MCAO models[26,44]. These findings highlight the therapeutic potential of developing isoform-specific HMGB1 inhibitors for the precise modulation of inflammatory responses in various disease contexts[24,45].

Despite compelling evidence of Ori's protective effect against cerebral I/R injury *via* HMGB1 binding, our study has limitations. First, the precise molecular mechanism by which Ori binds to HMGB1 to suppress its secretion and proinflammatory activity warrants further investigation. Second, the specific redox states (eg, disulfide *vs*. fully reduced) of extracellular HMGB1 modulated by Ori remain undefined; however, this is critical because these dictate its cytokine-inducing capacity. Finally, while our data strongly support HMGB1 as a primary target, the possible involvement of other off-target effects in Ori's neuroprotection merits further exploration. Therefore, future studies should focus on addressing these questions.

Conclusions

Our study demonstrated that Ori confers robust protection against cerebral I/R injury in both *in vitro* (OGD/R-induced neuronal injury) and *in vivo* (mouse tMCAO) models. Mechanistically, we identified that Ori directly and covalently bound to Cys106 of HMGB1 *via* its α, β-unsaturated carbonyl group (carbon–carbon double bond), thereby neutralizing the proinflammatory activity of HMGB1. Furthermore, Ori exerted multimodal anti-inflammatory effects by reducing HMGB1 secretion into the extracellular space, decreasing cytoplasmic HMGB1 accumulation, and suppressing the downstream HMGB1/TLR4/MyD88/NF-κB signaling cascade. These findings establish HMGB1 as a key therapeutic target for Ori and highlight its potential as a lead compound in IS treatment. Given the central role

of HMGB1 in sterile inflammation, our study suggests broader applications of Ori in other HMGB1-driven inflammatory disorders.

Conflict of interest statement

The authors declare no conflict of interest.

Funding

The project was financially supported by the National Natural Science Foundation of China (82204672), Scientific and technological innovation project of China Academy of Chinese Medical Sciences (CI2023E002, CI2023E005TS05, CI2023E005TS08), and the Fundamental Research Funds for the Central Public Welfare Research Institutes (ZZ15-YQ-063, ZZ15-YQ-064, ZZ14-YQ-050, and ZZ17-ND-10-10).

Author contributions

Dandan Liu contributed to methodology, formal analysis, writing-original draft, and resources. Shujie Zhang contributed to methodology, software, visualization, formal analysis, and investigation. Fei Xia and Yuqing Meng contributed to formal analysis and investigation. Qiaoli Shi contributed to visualization, formal analysis, and investigation. Hui Zhao and Yinkwan Wong contributed to formal analysis and software operation. Yanqing Liu, Yongping Zhu, Xin Chai, Jiale Xing, and Peili Wang contributed to formal analysis. Huan Tang contributed to supervision. Chong Qiu contributed to the investigation. Ang Ma contributed to writing-review and editing. Jigang Wang contributed to supervision and resources. All authors reviewed and approved the published version of the manuscript.

Ethical approval of studies and informed consent

All animal experiments were approved by the Animal Experimental Ethics Review Committee of the Institute of Chinese Materia Medica, China Academy of Chinese Medical Sciences (approval number: 2025B058), and met the requirements of the Beijing Administration Rule of Laboratory Animals.

Acknowledgments

None.

Data availability

All data generated or analyzed during this study are included in this published article.

Declaration of generative AI in scientific writing

The conception and writing of this article were carried out collaboratively by all authors. Artificial intelligence was utilized exclusively for refining sentence coherence and amending punctuation. All citations in this manuscript were manually searched for and incorporated. After utilizing the aforementioned tools/services, the authors thoroughly reviewed and revised the content and take full responsibility for the entirety of this publication.

References

[1] Vasu S, Luis G, Dileep RY. Global epidemiology of stroke and access to acute ischemic stroke interventions. *Neurology* 2021;97:S6–S16.
[2] Rabkin SW. Heart disease and stroke. *Heart Mind* 2023;7(3):115–116.
[3] Dmitry F, Alexander Z, Matthew B, et al. The development of novel drug treatments for stroke patients: a review. *Int J Mol Sci* 2022;23(10):5796.
[4] Shi K, Zou M, Jia DM, et al. tPA mobilizes immune cells that exacerbate hemorrhagic transformation in stroke. *Circ Res* 2021;128(1):62–75.
[5] Zhang M, Liu Q, Meng H, et al. Ischemia-reperfusion injury: molecular mechanisms and therapeutic targets. *Signal Transduct Target Ther* 2024;9(1):12.
[6] Alba S, Arthur L. Systemic inflammation after stroke: implications for post-stroke comorbidities. *EMBO Mol Med* 2022;14(9):e16269.
[7] Shi K, Tian DC, Li ZG, et al. Global brain inflammation in stroke. *Lancet Neurol* 2019;18(11):1058–1066.
[8] Tian XD, Liu CL, Shu Z, et al. Therapeutic targeting of HMGB1 in stroke. *Curr Drug Deliv* 2016;14(6):785–790.
[9] Li JM, Wang ZX, Li JM, et al. HMGB1: a new target for ischemic stroke and hemorrhagic transformation. *Transl Stroke Res* 2024;16(3):990–1015.
[10] Tao T, Liu MZ, Chen MY, et al. Natural medicine in neuroprotection for ischemic stroke: challenges and prospective. *Pharmacol Ther* 2020;216:107695.
[11] Lin R, Lin X, Wu J, et al. Inhibitory effects of in esophageal squamous cell carcinoma: network pharmacology and experimental validation. *Evid Based Complement Alternat Med* 2022;2022:2696347.
[12] Guo S, Cui X, Jiang M, et al. Simultaneous characterization and quantification of 17 main compounds in Rabdosia rubescens by high performance liquid chromatography. *J Food Drug Anal* 2017;25(2):417–424.
[13] Xu JM, Wold EA, Ding Y, et al. Therapeutic potential of oridonin and its analogs: from anticancer and antiinflammation to neuroprotection. *Molecules* 2018;23(2):474.
[14] Li X, Zhang CT, Ma W, et al. Oridonin: a review of its pharmacology, pharmacokinetics and toxicity. *Front Pharmacol* 2021;12:645824.
[15] Yan C, Yan H, Mao J, et al. Neuroprotective effect of oridonin on traumatic brain injury via inhibiting NLRP3 inflammasome in experimental mice. *Front Neurosci* 2020;14:557170.
[16] Greuel BK, Da Silva D, Robert-Gostlin V, et al. Natural compounds oridonin and shikonin exhibit potentially beneficial regulatory effects on select functions of microglia. *Brain Sci* 2024;14(4):328.
[17] Li L, Song JJ, Zhang MX, et al. Oridonin ameliorates caspase-9-mediated brain neuronal apoptosis in mouse with ischemic stroke by inhibiting RIPK3-mediated mitophagy. *Acta Pharmacol Sin* 2022;44(4):726–740.
[18] Liu DD, Luo P, Gu LW, et al. Celastrol exerts a neuroprotective effect by directly binding to HMGB1 protein in cerebral ischemia-reperfusion. *J Neuroinflammation* 2021;18(1):174.
[19] Yang T, Liu DD, Li Y, et al. Chemoproteomics reveals sofalcone inhibits the inflammatory response of Caco-2 cells by covalently targeting HMGB1. *Chem Commun (Camb)* 2023;59(58):8981–8984.
[20] Guo QY, Wang QX, Chen JY, et al. Dihydroartemisinin regulated the MMP-mediated cellular microenvironment to alleviate rheumatoid arthritis. *Research* 2024;7:0459.
[21] Lu Y, Shen ZX, Xu YP, et al. Discovery of new phenyltetrazolium derivatives as ferroptosis inhibitors for treating ischemic stroke: an example development from free radical scavengers. *J Med Chem* 2024;67(14):11712–11731.
[22] Hwang IC, Kim JY, Kim JH, et al. Therapeutic potential of a novel necrosis inhibitor, 7-amino-indole, in myocardial ischemia-reperfusion injury. *Hypertension* 2018;71(6):1143–1155.
[23] Ugrinova I, Pasheva E. HMGB1 protein: a therapeutic target inside and outside the cell. *Adv Protein Chem Struct Biol* 2017;107:37–76.

[24] Venereau E, De Leo F, Mezzapelle R, et al. HMGB1 as biomarker and drug target. *Pharmacol Res* 2016;111:534–544.
[25] Paudel YN, Angelopoulou E, Piperi C, et al. HMGB1-mediated neuroinflammatory responses in brain injuries: potential mechanisms and therapeutic opportunities. *Int J Mol Sci* 2020;21(13):4609.
[26] Andersson U, Tracey KJ. HMGB1 is a therapeutic target for sterile inflammation and infection. *Annu Rev Immunol* 2011;29:139–162.
[27] Shen LP, Yang JS, Zhu ZF, et al. Elevated serum HMGB1 levels and their association with recurrence of acute ischaemic stroke. *J Inflamm Res* 2024;17:6887–6894.
[28] Toshiyuki T, Ryu K, Mitsugu F, et al. Elevated serum high-mobility group box-1 protein level is associated with poor functional outcome in ischemic stroke. *J Stroke Cerebrovasc Dis* 2017;26(10):2404–2411.
[29] Owona BA, Schluesener HJ. Molecular insight in the multifunctional effects of oridonin. *Drugs R D* 2015;15(3):233–244.
[30] Liang L, Wang H, Hu Y, et al. Oridonin relieves depressive-like behaviors by inhibiting neuroinflammation and autophagy impairment in rats subjected to chronic unpredictable mild stress. *Phytother Res* 2022;36(8):3335–3351.
[31] Zhang ZY, Daniels R, Schluesener HJ. Oridonin ameliorates neuropathological changes and behavioural deficits in a mouse model of cerebral amyloidosis. *J Cell Mol Med* 2013;17(12):1566–1576.
[32] Wang SL, Yang H, Yu LJ, et al. Oridonin attenuates Aβ1-42-induced neuroinflammation and inhibits NF-κB pathway. *PLoS One* 2014;9(8):e104745.
[33] Li L, Cheng SQ, Guo W, et al. Oridonin prevents oxidative stress-induced endothelial injury via promoting Nrf-2 pathway in ischaemic stroke. *J Cell Mol Med* 2021;25(20):9753–9766.
[34] Tang D, Kang R, Zeh HJ, et al. The multifunctional protein HMGB1: 50 years of discovery. *Nat Rev Immunol* 2023;23(12):824–841.
[35] Harris HE, Andersson U, Pisetsky DS. HMGB1: a multifunctional alarmin driving autoimmune and inflammatory disease. *Nat Rev Rheumatol* 2012;8(4):195–202.
[36] Yu Y, Tang DL, Kang R. Oxidative stress-mediated HMGB1 biology. *Front Physiol* 2015;6:93.
[37] Andersson U, Tracey KJ, Yang H. Post-translational modification of HMGB1 disulfide bonds in stimulating and inhibiting inflammation. *Cells* 2021;10(12):3323.
[38] Ren W, Zhao L, Sun Y, et al. HMGB1 and Toll-like receptors: potential therapeutic targets in autoimmune diseases. *Mol Med* 2023;29(1):117.
[39] Le K, Mo S, Lu X, et al. Association of circulating blood HMGB1 levels with ischemic stroke: a systematic review and meta-analysis. *Neurol Res* 2018;40(11):907–916.
[40] E Y, Deng Q, Shi G, et al. The association between high mobility group box 1 and stroke-associated pneumonia in acute ischemic stroke patients. *Brain Sci* 2022;12(11):1580.
[41] Im KI, Kim N, Lim JY, et al. The free radical scavenger NecroX-7 attenuates acute graft-versus-host disease via reciprocal regulation of Th1/regulatory T cells and inhibition of HMGB1 release. *J Immunol* 2015;194(11):5223–5232.
[42] Singh V, Roth S, Veltkamp R, et al. HMGB1 as a key mediator of immune mechanisms in ischemic stroke. *Antioxid Redox Signal* 2016;24(12):635–651.
[43] Gao B, Wang SW, Li JF, et al. HMGB1, angel or devil, in ischemic stroke. *Brain Behav* 2023;13(5):e2987.
[44] Nishibori M, Mori S, Takahashi HK. Anti-HMGB1 monoclonal antibody therapy for a wide range of CNS and PNS diseases. *J Pharmacol Sci* 2019;140(1):94–101.
[45] Yang T, He YY, Huang MN, et al. Clinical study on the modulating effects of Jiaotaiwan on the microbiota–SCFAs–neurotransmitter/immune axis in patients with depression. *Acupunct Herb Med* 2025;5(4):456–468.